Theoretical and Experimental Study of the Factors Influencing Regio- and Stereochemical Control in the Reactions of Nucleophiles with Metal Carbonyl Complexes

David A. Brown,* John C. Burns, Paul C. Conlon, John P. Deignan, Noel J. Fitzpatrick, William K. Glass, and Patrick J. O'Byrne

Department of Chemistry, University College, Belfield, Dublin 4, Ireland

Received December 15, 1995[⊗]

The factors influencing the regio- and stereochemical control of reactions between phosphines and phosphites with (A) a series of tricarbonyl(η^7-tropylium)metal cations (M = Cr, Mo, W) and (B) a series of tricarbonyl(η^6-substituted arene)manganese cations (substituent = Cl, Me, p-Me_2, 1,3,5-Me_3) are examined theoretically using the interaction determinant method of calculating interaction energies and experimentally using low-temperature infrared and ^{1}H NMR spectroscopy to identify the nature of the initial attack site in the substrate. In all cases the reactions are predicted to be orbitally controlled and agreement is found between calculated site−nucleophile interaction energies and observed initial attack site both in terms of stereochemistry, e.g. exo ring attack is predicted correctly over endo ring attack, and regioselectivity, e.g. $P(OMe)_3$ is predicted correctly to give metal attack with the molybdenum and tungsten tropylium complexes.

The ability of metal carbonyls to undergo carbonyl substitution by nucleophiles is one of the reactions forming the basis of organometallic chemistry.[1] With the discovery of metal carbonyl complexes of π-acids, e.g. the stable $Cr(CO)_3$ complexes of arenes,[2] it was soon noted that complexation results in activation of arenes to nucleophilic substitution, a classic case being the ready substitution of chlorine in (η^6-C_6H_5Cl)$Cr(CO)_3$ by methoxide to give (η^6-C_6H_5OMe)$Cr(CO)_3$.[2,3] However, nucleophiles may also form ring adducts by simple addition to the π-acid ring often with high regio- and stereochemical control with the most common pathway being addition of the nucleophile to the exo face of the arene and formation of the corresponding η^5-cyclohexadienyl complexes.[4] Subsequent oxidation removes the $Cr(CO)_3$ group to give, in the case of carbanion nucleophiles, a substituted arene containing a new C−C bond. This reaction has proved to be of wide synthetic use in the formation of C−C bonds.[5] Similar synthetic uses of the related η^5-cyclohexadienylium and η^5-cycloheptadienylium iron tricarbonyl cations have been developed again with wide applications especially in natural product chemistry.[6] In view of these extensive synthetic uses of nucleophilic addition to π-acid metal carbonyl complexes, it is important to assess the various factors which influence regio- and stereochemical control of these reactions, for example, the factors which cause a nucleophile to form a ring adduct with a given substrate under one set of conditions (solvent, temperature, etc.) and a carbonyl substitution product under another set (solvent, temperature, etc.).

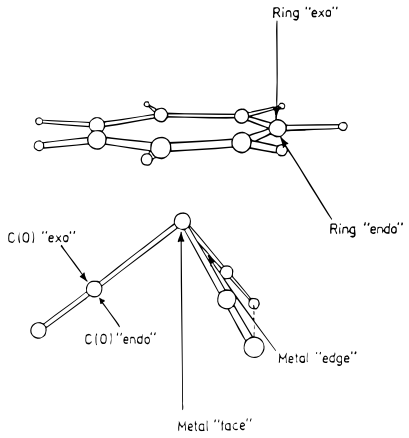

Figure 1. Geometries of the nucleophile−substrate system corresponding to ring, metal, and carbonyl attack.

In principle, the reaction between a nucleophile and a π-acid metal carbonyl complex may proceed by a number of pathways (Figure 1) to give a variety of products, including ring adducts, carbonyl substitution and addition products, and substituted metal carbonyls following metal−ring bond fission. In some instances, a number of the initial adducts may be of similar energies and their possible isolation as kinetic products at low temperatures, as distinct from intermediates, will depend upon the nature and availability of subsequent reaction pathways. For example, hydride addition from BH_4^- on [(η^5-C_5H_5)$Fe(CO)_3$]$^+$ at −80 °C proceeds via initial formation of the metal formyl, (η^5-C_5H_5)$Fe(CO)_2$(CHO), by attack at a carbonyl carbon atom,[7,8] for which

[⊗] Abstract published in *Advance ACS Abstracts,* June 1, 1996.

(1) Hardie, I.; Zuckemann, J. J. *Basic Organometallic Chemistry*; Walter Cruyter: Berlin, 1985.
(2) Nicholls, B.; Whiting, M. C. *J. Chem. Soc.* **1959**, 551.
(3) Brown, D. A.; Raju, J. R. *J. Chem. Soc. A* **1966**, 40.
(4) Card, R. J.; Trahanovsky, W. S. *Tetrahedron Lett.* **1973**, 3823.
(5) Semmelhack, M. F. In *Organic Synthesis: Today, Tomorrow*; Trost, B. M., Hutchinson, C. R., Eds.; 3rd IUPAC Symposium on Organic Synthesis; Pergamon: Oxford, U.K., 1981; p 63.
(6) For a review see: Pearson, A. J. *Compr. Org. Synth.* **1991**, *4*, 663.
(7) Brown, D. A.; Glass, W. K.; Mustafa, T. U. *Inorg. Chim. Acta* **1984**, *89*, L47.
(8) Brown, D. A; Glass, W. K; Salama, M. M. *J. Organomet. Chem.* **1994**, *474*, 129.

S0276-7333(95)00962-9 CCC: $12.00

Table 1. Parameters Used in Extended Hückel Calculations

	exponents				VOIPS (eV) (noniterated)			VOIPS (eV) (iterated)		
atom	*n*	*n*s	*n*p	$(n-1)$d	*n*s	*n*p	$(n-1)$d	*n*s	*n*p	$(n-1)$d
Cr	4	1.315	0.924	3.119	−6.59	−3.52	−7.785	−9.50	−6.88	−11.06
Mo	5	1.48	1.072	2.260	−6.571	−4.20	−8.394	−10.16	−6.37	−13.3
W	6	1.795	1.271	3.064	−6.5(a)	−4.2[a]	−8.4[a]	−10.57	−6.693	−12.96
C	2	1.553	1.45		−20.31	−10.71				
O	2	2.163	2.17		−32.34	−15.8				
H	1	1.30								

[a] Initial VOIPs approximated by values for molybdenum.

a ready decomposition pathway is available via loss of CO and formation of the corresponding metal hydride, $(\eta^5\text{-}C_5H_5)Fe(CO)_2H$, whereas, in contrast, addition of a phosphine, e.g. PEt_3, to $[(\eta^6\text{-}C_6H_6)Mn(CO)_3]PF_6$ at −40 °C gives the ring adduct $[(\eta^5\text{-}C_6H_6\text{-}exo\text{-}PEt_3)Mn(CO)_3]PF_6$, for which no facile decomposition pathway is available. Thus, a "dead-end" equilibrium is set up, so that on raising the temperature the ring adduct re-forms the starter cation which then reacts by the higher energy pathway of carbonyl substitution to form $[(\eta^6\text{-}C_6H_6)Mn(CO)_2(PEt_3)]PF_6$.[9]

Early attempts to understand the factors influencing the choice of reaction pathway were based on simple electrostatics i.e. on the assumption that the reaction was charge controlled and so the center with the highest positive charge (calculated by simple MO methods, such as the extended Hückel method, EHMO) would be the site of attack. Alternatively, if the reaction was assumed to be orbitally controlled, then the value of the square of the coefficient of the LUMO, the frontier orbital, at a particular site (A), P_A^{LUMO}, was used as a criterion for the point of attack.[10,11] Although qualitatively useful in certain cases, these approaches lack a sound theoretical basis; in particular, the fact that many metal carbonyl complexes of π-acids contain a group of unoccupied molecular orbitals (UMOs) lying within an energy band of 1−2 eV means that simple predictions based on the form of the frontier LUMO only are unlikely to be correct. For these reasons, we developed the interaction determinant method (IDM) of calculating, within an extended Hückel MO framework,[12] the interaction energy, ΔE_{RS}, between a particular nucleophile (S) and a given metal carbonyl complex (R) as substrate.[13] This method allows one to calculate interaction energies for various attack sites, pathways, and interaction distances, together with investigating the effect on ΔE_{RS} of variations in size of the frontier orbital sets of the reactants which overlap. Finally, solvent effects are included by addition of electrostatic terms involving the macroscopic dielectric constant. A similar approach has been developed by Weber and co-workers and applied successfully to discuss the sequential addition of a carbanion nucleophile to $(\eta^6\text{-}C_6H_6)Cr(CO)_3$.[14]

In principle, the most satisfactory theoretical approach involves full ab initio calculations of the energies of various intermediates and stable products together with transition states, but for reactions of large nucleophiles, such as the phosphines and phosphites discussed below, the ab initio approach is still not practicable; however for smaller molecules such as carbon monoxide, hydride, and methanol, ab initio methods have already proved to be effective in discussing reaction mechanisms. For example, an ab initio MO study of possible stereochemical reaction paths for methanol dehydrogenation by $Ru(OAc)Cl(PEtPh_2)_3$ was modeled successfully by $Ru(OAc)Cl(PH_3)_3$ and gave good agreement with experiment.[15] Within our group, ab initio calculations of the energies of various possible products formed by hydride attack on $[(\eta^5\text{-}C_5H_5)Fe(CO)_3]^+$ [16] correlated well with the low-temperature spectroscopic studies.[7,8]

In the present paper, we discuss the regio- and stereochemical selectivity shown in the reactions of phosphines (PH_3 and PMe_3) and phosphites ($P(OMe)_3$) with (A) a series of $[(\eta^7\text{-tropylium})M(CO)_3]BF_4$ complexes with M = Cr (**I**), Mo (**II**), and W (**III**) and (B) a series of $[(\eta^6\text{-substituted arene})Mn(CO)_3]PF_6$ complexes, $[(\eta^6\text{-}C_6H_{6-n}Me_n)Mn(CO)_3]PF_6$ ($n = 1$ (**IV**), $n = 2$ (**V**), $n = 3$ (**VI**)) and $[(\eta^6\text{-}C_6H_5Cl)Mn(CO)_3]PF_6$ (**VII**), with reference to the effects on regio- and stereochemical selectivity of substitution of the arene in series B and variation of M and solvent in series A. Interaction energies calculated by the IDM approach are compared with experimental synthetic studies and variable-temperature infrared and ^1H and ^{13}C NMR spectroscopy.

Computational Methods

The interaction energy was calculated using a program developed at University College Dublin[13] which uses as input the results from iterative EHMO calculations[12] on the supermolecule RS. Separate iterative calculations on R and S are also used. The geometries of the nucleophiles and substrates in the supermolecules (RS) were considered to be those of the isolated species. In the iterative calculations on R, S, and RS the diagonal terms were represented by valence orbital ionization potentials (VOIPs).[17,18] The off-diagonal terms were calculated using the weighted Wolfsberg−Helmholz approximation.[19] The exponents used were those of Fitzpatrick and Murphy.[20] Parameters used are summarized in Table 1. Calculations at distances of 2 and 3 Å between the phosphorus atom of the nucleophile and the substrate atom being attacked were considered. In both cases the trends in results were similar; thus the latter are reported. The results were insensitive to slight angular variations, thus the attack trajectories in Figure 1 were considered. The calculations of

(9) Brown, D. A.; Glass, W. K.; Kreddan, K. M. *J. Organomet. Chem.* **1991**, *413*, 233.
(10) Hudson, R. F. In *Chemical Reactivity and Reaction Rates*; Klopman, G., Ed.; Wiley: New York, 1974; Chapter 5.
(11) Fukui, K. *Reactivity and Structure Concepts in Organic Chemistry*; Springer Verlag: New York, 1975.
(12) Howell, J.; Rossi, A.; Wallace, D.; Haraki, K.; Hoffmann, R. *QCPE* **1977**, No. *344*.
(13) Brown, D. A.; Fitzpatrick, N. J.; McGinn, M. A. *J. Organomet. Chem.* **1985**, *239*, 235.
(14) Weber, J.; Stussi, D.; Fluekiger, P.; Margantini, P. Y. *Comments Inorg. Chem.* **1992**, *14*, 27.
(15) Itagaki, H.; Koga, N.; Morokuma, K.; Saito, Y. *Organometallics* **1993**, *12*, 1648.
(16) Brown, D. A.; Fitzpatrick, N. J.; Groarke, P. J.; Koga, N.; Morakuma, K. *Organometallics* **1993**, *12*, 2521.
(17) Basch, H.; Viste, A.; Gray, H. B. *Theor. Chim. Acta* **1965**, *3*, 458.
(18) Munita, R.; Letelier, J. R. *Theor. Chim. Acta* **1981**, *58*, 167.
(19) Wolfsberg, M.; Helmholz, L. *J. Chem. Phys.* **1952**, *20*, 837.
(20) Fitzpatrick, N. J.; Murphy, G. H. *Inorg. Chim. Acta* **1984**, *87*, 41.

ΔE_{RS} were also based on the program of Hoffmann and coworkers.[12] Thus this perturbation method, based on EH theory, is computationally inexpensive and readily applied to inorganic systems. It allows both the nature of the solvent and the nucleophile to be explicitly considered.

$$\Delta E_{RS} = \Delta E_{RS(solvation)} + \Delta E_{RS(orbital)}$$

$$\Delta E_{RS(solvation)} = \sum q_r q_s/(R_{rs}\epsilon)$$

where q_r and q_s are the charges, R_{rs} is the internuclear distance, and ϵ is the dielectric constant. In the calculation of $\Delta E_{RS(orbital)}$ the levels of RS are populated from the MOs of R and S. The determinant may include as many MOs on R and S as desired.

Two ranges of orbitals were considered. The first is based on moving 1 eV from the LUMO and HOMO, and the second, on moving 2 eV from these orbitals. No changes in the order of interaction energies were observed. Thus the second series of occupied and unoccupied orbitals was used. Both PMe_3 and $P(OMe)_3$ were considered as pure nucleophiles, since the HOMO−LUMO gap in each case is greater than 12 eV (see Supporting Information).

Results and Discussion

A. Nucleophilic Attack by PMe_3 and $P(OMe)_3$ on $[(\eta^7\text{-}C_7H_7)M(CO)_3]BF_4$ (I, M = Cr; II, M = Mo; III, M = W). Theoretical Results. Interaction energies (ΔE_{RS}) calculated by the IDM method as described above for attack by both PMe_3 and $P(OMe)_3$ on **I**−**III** are given in Table 2. The possible sites of attack for which ΔE_{RS} was calculated are illustrated in Figure 1. As previously noted, in all cases ΔE_{RS} was calculated for a distance of 3 Å between the phosphorus atom and the atom of the complex being attacked (ring carbon, metal, and carbonyl carbon) which corresponds to an early transition state for both ring-carbon attack (equilibrium distance = 1.86 Å [21]) and metal attack (equilibrium distance ≈ 2.2−2.3 Å [22]). Correlation can then be made between the calculated interaction energies in Table 2 and the site of initial attack (kinetic products) summarized in Table 3. As mentioned in the introduction, one of the difficulties of using simple reactivity criteria such as P_A^{LUMO} to predict the site of nucelophilic attack on a complex such as the cation $[(\eta^7\text{-}C_7H_7)M(CO)_3]^+$ is the occurrence of a band of UMOs in such systems. Accordingly, ΔE_{RS} values were calculated at 3 Å for both a small group of MOs (set a) and a larger group (set b) as described in the computational section above. No change in order of attack site was observed between the two sets so, for clarity, only one (set b) is given in Table 2. Solvent effects were estimated by calculating the electrostatic terms for solvents of low dielectric constant ($\epsilon = 2$) and high dielectric constant ($\epsilon = 100$), columns 3−6 of Table 2). Finally, for convenience only relative interaction energies are given in Table 2, based on the lowest calculated ΔE_{RS} set to zero for each series. However the actual values corresponding to these relative zero values are included in the table.

Before consideration of the theoretical results in detail, a number of general conclusions emerge from the calculated interaction energies. First, these reactions are predicted to be orbitally controlled since the order of calculated interaction energies between different sites in the complete series (**I**−**VII**), including both the tropylium and arene complexes, does not, in general, vary between the cases with $\epsilon = 2$ and $\epsilon = 100$. Second, for both series of complexes, the calculated interaction

Table 2. Calculated Relative Interaction Energies (ΔE_{RS}) between PMe_3 and $P(OMe)_3$ and the Cations of (A) $[(\eta^7\text{-}C_7H_7)M(CO)_3]BF_4$ (M = Cr, Mo, W (I−III)) and (B) (Substituted arene)tricarbonylmanganese Complexes $[(\eta^6\text{-}C_6H_{6-n}Me_n)Mn(CO)_3]PF_6$ (n = 1 (IV); n = 2 (V); n = 3 (VI) (PH_3 only)) and $[\eta^6\text{-}C_6H_5Cl)Mn(CO)_3]PF_6$ (VII)

		PMe_3		$P(OMe)_3$	
complex	attack site	$\epsilon = 2$	$\epsilon = 100$	$\epsilon = 2$	$\epsilon = 100$
I	ring exo	18.6	16.1	15.4	13.7
	ring endo	14.8	13.4	14.7	13.6
	metal face	16.3	15.1	16.5	13.7
	metal edge	15.6	14.0	16.0	13.6
	carbonyl exo	14.9	13.0	14.6	13.0
	carbonyl endo	14.9	13.4	15.7	13.9
II	ring exo	6.6	4.8	2.0	0.6
	ring endo	4.5	0.4	3.0	1.0
	metal face	6.3	2.8	5.4	3.1
	metal edge	4.7	1.5	4.0	1.7
	carbonyl exo	3.1	0.0[a]	2.7	0.3
	carbonyl endo	4.1	0.8	3.0	1.1
III	ring exo	6.0	4.0	2.2	0.3
	ring endo	4.6	2.0	2.4	1.3
	metal face	5.8	2.7	5.3	3.2
	metal edge	4.6	1.0	4.0	1.9
	carbonyl exo	3.1	0.0	2.6	0.3
	carbonyl endo	4.1	1.1	3.2	1.1
IV	C_1 exo	9.4	8.3	6.9	6.0
	C_1 endo	9.2	8.2	6.3	5.4
	C_2 exo	11.3	10.7	7.3	6.6
	C_2 endo	10.0	9.2	7.0	5.6
	C_3 exo	13.6	12.2	8.2	7.3
	C_3 endo	12.3	11.0	7.3	6.2
	C_4 exo	10.6	8.9	7.4	6.6
	C_4 endo	9.5	8.3	6.7	5.7
	metal face	9.1	8.0	12.5	11.8
	metal edge	5.8	4.7	10.4	10.0
	carbonyl exo	3.4	2.5	7.0	5.6
	carbonyl edge	2.9	1.8	6.1	4.8
V[b]	C_1 exo	10.4	8.9	8.7	8.7
	C_1 endo	10.0	8.7	7.3	6.4
	C_2 exo	12.6	10.5	10.3	8.7
	C_2 endo	11.3	9.6	7.9	7.0
	metal face	10.1	8.8	8.1	7.7
	metal edge	7.7	5.1	4.6	2.6
	carbonyl exo	2.3	1.5	1.6	0.1
	carbonyl endo	2.2	1.5	1.3	0.0[c]
VI[d]	C_1 exo	4.4	2.6		
	C_1 endo	4.1	2.4		
	C_2 exo	4.8	4.1		
	C_2 endo	4.5	3.2		
	metal face	11.0	9.3		
	metal edge	6.7	5.0		
	carbonyl exo	2.3	1.5		
	carbonyl endo	2.3	1.3		
VII	C_1 exo	13.0	12.2	8.0	7.6
	C_1 endo	12.3	11.5	7.4	6.5
	C_2 exo	15.2	14.4	7.7	7.0
	C_2 endo	14.6	13.2	6.7	5.9
	C_3 exo	15.3	14.3	9.5	8.4
	C_3 endo	14.5	13.6	8.8	7.7
	C_4 exo	14.0	13.2	8.2	7.4
	C_4 endo	13.1	12.6	7.6	7.0
	metal face	11.4	10.9	9.7	9.3
	metal edge	10.5	9.7	9.7	9.2
	carbonyl exo	8.3	7.3	7.6	6.7
	carbonyl edge	7.4	6.6	7.3	6.3

[a] For η^7 complexes 0.0 corresponds to 24.87 eV. [b] Values in columns 5 and 6 are for PH_3 (not $P(OMe)_3$). [c] For η^6 complexes 0.0 corresponds to 2.65 eV. [d] Values in columns 3 and 4 are for PH_3 (not PMe_3).

(21) Brown, D. A.; Burns, J. C.; Glass, W. K.; Cunningham, D.; Higgins, T.; McArdle, P.; Salama, M. M. *Organometallics* **1994**, *13*, 2662.

(22) Lee, K. J.; Brown, T. L. *Inorg. Chem.* **1992**, *31*, 289.

Table 3. Initial Attack Sites and Thermodynamic Products of the Reactions of PR_3 with (A) $[(\eta^7\text{-}C_7H_7)M(CO)_3]BF_4$ (M = Cr, Mo, W (I−III); R = Me, OMe) and (B) $[(\eta^6\text{-}C_6H_{6-n}Me_n)Mn(CO)_3]PF_6$ (n = 1 (IV); n = 2 (V); n = 3 (VI)) and $[(\eta^6\text{-}C_6H_5Cl)Mn(CO)_3]PF_6$ (VIII)[a]

		initial attack site (low temps)		thermodynamic product	
complex	solvent	PMe_3	$P(OMe)_3$	PMe_3	$P(OMe)_3$
I	THF	metal	metal	ring D	ring D
	EtOH	ring A	ring A	ring A	ring A
	toluene	metal	metal	ring D	ring D
II, III	THF	metal	metal	ring D	ring D
	EtOH	ring A	metal	ring A	ring D, CO sub
	toluene	metal	metal	CO sub	CO sub
IV	acetone	ring A (meta addn)	no reacn	CO sub	CO sub
V	acetone	ring A	no reacn	CO sub	CO sub
VI	acetone	no reacn	no reacn	CO sub	CO sub
VII	acetone	Ring A (o:m = 2:1)	no reacn	ring D	CO sub

[a] Ring A = $[(\eta^6\text{-}C_7H_7\text{-}exo\text{-}PR_3)M(CO)_3]BF_4$ (R = Me, OMe; M = Cr, Mo, W), $[(\eta^5\text{-}C_6H_{6-n}Me_n\text{-}exo\text{-}PR_3)Mn(CO)_3]PF_6$ (R = Me, Et;[9] n = 1, 2), and $[(\eta^5\text{-}C_6H_5Cl\text{-}exo\text{-}PR_3)Mn(CO)_3]PF_6$ (R = Me, Et[9]). Ring D = $(PR_3)_3M(CO)_3$ (R = Me, OMe; M = Cr, Mo, W) and *fac*-$Mn(CO)_3(PR_3)_2Cl$ (R = Me, Et[9]). CO sub = $[(\eta^7\text{-}C_7H_7)M(CO)_2PR_3]BF_4$ (R = Me, OMe; M = Mo, W), $[(\eta^6\text{-}C_6H_{6-n}Me_n)Mn(CO)_2PR_3]PF_6$ (R = Me, OMe; n = 1−3), and $[(\eta^6\text{-}C_6H_5Cl)Mn(CO)_2P(OMe)_3]PF_6$.

energies for exo ring attack are generally greater than for ring endo attack (Table 2) and thus the IDM approach gives theoretical support to the generally observed preference for ring exo attack.[23] Third, again for both series of complexes (**I**−**III**, **IV**−**VII**), ΔE_{RS} for exo ring attack by PMe_3 is greater than for the analogous reaction with $P(OMe)_3$. This is consistent with the reduced nucleophilicity of phosphite ligands to carbon-based electrophiles as reflected in the HOMO phosphorus electron densities for PMe_3 and $P(OMe)_3$ of 0.739 and 0.373, respectively. However, although the calculated ΔE_{RS} values for PMe_3 and $P(OMe)_3$ exo attack at the ring carbon atoms of **I**−**III** follow accepted views of their relative nucleophilicities, the ΔE_{RS} values for metal attack show less variation. For example, for **I**, $[(\eta^7\text{-}C_7H_7)Cr(CO)_3]BF_4$, ΔE_{RS} for ring exo attack by PMe_3 is 16.1 (ϵ = 100) compared to 13.7 for $P(OMe)_3$ (ϵ = 100), whereas for metal face attack the respective values are 15.1 and 13.7. The corresponding values for edge attack are 14.0 and 13.6. We suggest that the reason for both the lower value of ΔE_{RS} for metal attack as against exo ring attack and the smaller variation with nucleophilicity of the attacking species lies with the greater importance of HOMO-HOMO repulsion between the nucleophile and the metal complex for the metal attack pathway. MO calculations[24] on $[(\eta^7\text{-}C_7H_7)Cr(CO)_3]^+$ indicate that of the group of five highest occupied orbitals three of these contain approximately 80% contributions from the $Cr(CO)_3$ moiety, resulting in the metal attack pathway suffering considerable repulsion for both PMe_3 and $P(OMe)_3$, a repulsion which will be largely absent for ring exo attack. In further support of this argument, it will be noted that interaction energies calculated for metal attack for the molybdenum complex (**II**) are much lower than for the analogous chromium complex (**I**) despite the orbital extension expected for a second-row transition element. Again MO calculations for **II** are revealing and show that now *all* the OMOs of **II**, used in the calculation of ΔE_{RS}, contain approximately 90% contributions from the $Mo(CO)_3$ moiety, thereby leading to increased repulsions between the metal center and both phosphine and phosphite nucleophiles (see Supporting Information). It is of interest to note that previous calculations of ΔE_{RS} between the much smaller methoxide ion and **I**−**III** predicted initial attack at the $M(CO)_3$ moiety rather than ring addition,[25] in agreement with low temperature spectroscopic studies[26] and subsequent kinetic studies.[27]

In more detail, the calculated interaction energies between PMe_3 and the complexes, **I**−**III** in polar solvents (ϵ = 100) predict ring exo attack in all cases due to the presence of ring-centered UMOs in this series and the absence of the OMO−OMO repulsion for this pathway of attack as discussed above. In the case of $P(OMe)_3$ metal attack is not strongly favored for the chromium complex (**I**) but it is for the molybdenum and tungsten complexes (**II** and **III**), presumably because the interaction of the weaker nucleophile $P(OMe)_3$ with ring-centered UMOs is lower than its interaction with metal-centered orbitals, despite the OMO−OMO repulsion.

Experimental Results. The experimental results showing the initial attack sites (kinetic products) together with the final thermodynamic products are summarized in Table 3 for a range of solvents. The initial products were identified by carrying out the reactions at −78 °C and the use of low-temperature infrared and NMR spectroscopy. Thermodynamic products were isolated and characterized by analysis and spectroscopy. Selected data are given in Tables 4 and 5 and the remainder in the Supporting Information.

It should be noted that the entry "ring" in Table 3 under the initial attack columns means that clear infrared (and often ^{1}H NMR) evidence was obtained at −78 °C for the ring adduct. The entry "metal" means that no evidence was obtained for ring attack, but subsequent formation of the final thermodynamic product involving either carbonyl substitution or ring−metal bond fission occurred, which involves metal attack.

Reactions of PR_3 (R = Me, OMe) with $[(\eta^7\text{-}C_7H_7)Cr(CO)_3]BF_4$ (Species I). Addition of $P(OMe)_3$ to a slurry of **I** in ethanol at −78 °C led to a slow color change from orange to dark red and the appearance of three new ν(CO) peaks at 1990, 1930, and 1900 cm^{-1}, close to those previously reported for $[(\eta^6\text{-}C_7H_7\text{-}exo\text{-}P(n\text{-}Bu)_3Cr(CO)]BF_4$.[28] The ^{1}H NMR spectrum confirmed

(23) Pauson, P. L. *J. Organomet. Chem.* **1980**, *200*, 207.
(24) Mealli, K.; Proserpio, D. M. *J. Chem. Educ.* **1990**, *67*, 399.
(25) Brown, D. A.; Fitzpatrick, N. J.; McGinn, M. A.; Taylor, T. H. *Organometallics* **1986**, *5*, 152.
(26) Brown, D. A.; Fitzpatrick, N. J.; Glass, W. K.; Taylor, T. H. *Organometallics* **1986**, *5*, 158.
(27) Powell, P.; Stephens, M.; Yassin, K. H. *J. Organomet. Chem.* **1986**, *301*, 313.
(28) Hackett, P.; Jaouen, G. *Inorg. Chim. Acta* **1976**, *12*, L19.

Table 4. Selected Analytical Data and Infrared Carbonyl Stretching Frequencies for Kinetic and Thermodynamic Products from the Reactions of PMe_3 and $P(OMe)_3$ with (A) [(η^7-C_7H_7)M(CO)$_3$]BF_4 (M = Cr, Mo, W) and (B) (Substituted arene)tricarbonylmanganese Complexes, [(η^6-$C_6H_{6-n}Me_n$)Mn(CO)$_3$]PF_6 (n = 2, 3) and [(η^6-C_6H_5Cl)Mn(CO)$_3$]PF_6

complex	calcd (%) C	calcd (%) H	calcd (%) P	found (%) C	found (%) H	found (%) P	ν(CO), cm^{-1}
[(η^6-C_7H_7-*exo*-PMe_3)Cr(CO)$_3$]BF_4 (**VIII**)	40.1	4.1	7.9	40.6	4.2	8.3	1990, 1935, 1905
[(η^6-C_7H_7-*exo*-P(OMe)$_3$)Cr(CO)$_3$]BF_4 (**IX**)	35.7	3.7	7.1	36.0	3.9	6.9	1990, 1930, 1900
fac-(PMe_3)$_3$Cr(CO)$_3$ (**X**)	39.6	7.4	25.5	40.3	7.3	26.6	1939, 1849
[(η^6-C_7H_7-*exo*-PMe_3)Mo(CO)$_3$]BF_4 (**XI**)	36.1	3.7	7.1	36.8	4.1	6.9	1998, 1936, 1901
fac-(P(OMe)$_3$)Mo(CO)$_3$ (**XII**)							1945, 1854
[(η^7-C_7H_7)Mo(CO)$_2$P(OMe)$_3$]BF_4 (**XIII**)	31.8	3.5	6.8	31.7	3.6	7.0	2035, 1996
[(η^5-$C_6H_4Me_2$-*exo*-PMe_3)Mn(CO)$_3$]PF_6 (**XIV**)							2019, 1940
[(η^6-$C_6H_4Me_2$)Mn(CO)$_2$$PMe_3$)]$PF_6$ (**XV**)	28.8	3.3		29.0	3.41		1990, 1942
[(η^6-$C_6H_4Me_2$)Mn(CO)$_2$P(OMe)$_3$]PF_6 (**XVI**)							2008, 1962
[(η^6-$C_6H_3Me_3$)Mn(CO)$_2$$PMe_3$]$PF_6$ (**XVII**)	35.8	4.52		35.5	4.32		1988, 1938
[(η^6-$C_6H_3Me_3$)Mn(CO)$_2$P(OMe)$_3$]PF_6 (**XVIII**)							2003, 1958

Table 5. ^{1}H Spectral Data for Selected Complexes[a]

complex	chem shifts (δ, ppm)	assgnts
VIII	5.70 (dt), J_{67} = 9.0	H_7
	5.54 (dt)	$H_{3,4}$
	5.01 (dt)	$H_{2,5}$
	3.56 (dt)	$H_{1,6}$
	2.55 (s)	CH_3
IX	6.10 (dt), $J_{6,7}$ = 8.0	H_7
	5.84 (dt)	$H_{3,4}$
	5.31 (dt)	$H_{2,5}$
	4.14 (dt)	$H_{1,6}$
	2.97 (s)	CH_3
XIII	5.64 (d), J = 2.7	ring protons (C_7H_7)
	4.08 (s)	OMe
XIV	5.89 (br)	H_3
	5.12 (d), $J_{3,4}$ = 4.78	H_4
	3.50 (m)	H_2
	3.99 (m)	H_1
	2.01 (s)	$CH_3(\alpha)$
	1.70 (s)	$CH_3(\beta)$
	1.57 (d), J_{P-CH_3} = 13.9	PMe_3
XV	5.93 (d), J_{P-H} = 2.6	ring protons
	2.27 (s)	CH_3
	1.59 (d)	PMe_3
XVI	6.18 (s)	ring protons
	2.20 (s)	ring methyls
	1.75 (d), J_{P-CH3} 10.5	PMe_3

[a] J values in Hz.

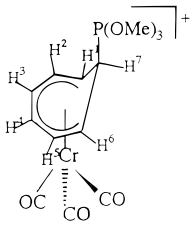

Figure 2. Labeling of [(η^6-C_7H_7-*exo*-P(OMe$_3$))Cr(CO$_3$)]$^+$.

formation of an exo ring adduct with ring proton resonances at δ 6.10 (dt, H_7), δ 5.84 (dt, $H_{3,4}$), δ 5.31 (dt, $H_{2,5}$), and δ 4.14 (dt, H_1), (Tables 4 and 5; Figure 2). The value of $J_{6,7}$ of 8.0 Hz confirms the exo stereochemistry of the ring adduct so formed, [(η^6-C_7 H_7-*exo*-P(OMe$_3$)Cr(CO$_3$]BF_4. On an increase of the temperature, the adduct remained stable. Analytical results are given in Table 4.

Reaction with PMe_3 occurred similarly to give the ring adduct but at a much faster rate. Selected analytical and spectroscopic data are given in Tables 4 and 5 and in the Supporting Information.

Effect of Solvent. In THF, the above reaction of **I** with both PMe_3 and $P(OMe)_3$ at −78 °C gave no evidence for ring addition, but slow formation of the ring-displaced products, *fac*-(PR_3)$_3$Cr(CO)$_3$ (R = Me, OMe), occurred identified by analysis and spectroscopy (Table 4). In toluene, the same reactions occurred but only on warming to 40 °C.

Reactions of PR_3 (R = Me, OMe) with Species II and III. Addition of PMe_3 to a slurry of **II** in ethanol at −78 °C gave an immediate color change from orange to red and formation of the violet ring adduct, [(η^6-C_7H_7-*exo*-PMe_3)Mo(CO$_3$]BF_4, characterized by analysis and spectroscopic methods (Tables 4 and 5). Species **III** behaved similarly.

In contrast, reaction of **II** with $P(OMe)_3$ in ethanol at −78 °C gave no evidence for ring addition, but instead formation of the carbonyl-substituted product (indicating metal attack), [(η^7-C_7H_7)Mo(CO)$_2$P(OMe)$_3$]BF_4, and the ring-displaced product, *fac*-(P(OMe)$_3$)$_3$Mo(CO)$_3$, occurred (Tables 4 and 5). Species **III** behaved similarly.

Effect of Solvent. In THF, reaction of **II** and **III** with both PMe_3 and $P(OMe)_3$ occurred rapidly, even at −78 °C with formation of the ring displaced products only, *fac*-(PR_3)$_3$M(CO)$_3$ (M = Mo, W; R = Me, OMe), probably due to the strong donor character of THF leading to metal attack and gradual reduction in ring hapticity and subsequent fission of the metal−ring bond and ring displacement, as suggested for displacement of the ring in this series by acetonitrile.[29] This result shows that specific solvation effects may play an important role in influencing the mechanism of the reaction between a nucleophile and this series (**I**−**III**). Such effects cannot be included within the IDM approach. In toluene, as in the case of **I**, no reaction occurred at low temperatures, but on the increase of the temperature, **II** and **III** gave the carbonyl substitution products [(η^7-C_7H_7)M(CO)$_2$$PR_3$]$BF_4$ (M = Mo, W; R = Me, OMe), rather than the ring-displaced product given by **I** in toluene.

Comparison between Theoretical and Experimental Results. In general there is agreement between the calculated interaction energies ΔE_{RS} given in Table 2 and the pattern of reaction products shown in Table 3. The IDM approach predicts correctly that PMe_3 will give ring addition as the initial product for all three complexes and, moreover, correctly predicts that for $P(OMe)_3$ metal attack is not strongly favored in the chromium complex (**I**), while it is in the cases of the molybdenum and tungsten complexes (**II** and **III**), which is consistent with the absence of ring attack for **II** and **III** at low temperatures and formation of both ring-displaced and carbonyl substitution products as the

(29) Al-Kathumi, K. M.; Kane-Maguire, L. A. P. *J. Chem. Soc., Dalton Trans.* **1973**, 1683.

final stable products of the reaction. The method is not so successful in discussing solvent effects, especially if specific solvation by a donor solvent such as THF is involved in the actual reaction mechanism.

B. Nucleophilic Attack by PR_3 on $[(\eta^6\text{-}C_6H_{6-n}Me_n)Mn(CO)_3]PF_6$ (n =1 (IV), R = Me, OMe; n = 2 (V), R = H, Me, OMe; n = 3 (VI), R = H, Me, OMe) and $[(\eta^6\text{-}C_6H_5Cl)Mn(CO)_3]PF_6$, (VII) (R = Me, OMe). In part B, we discuss the application of the IDM approach to the calculation of interaction energies, ΔE_{RS}, between the phosphines, PH_3 and PMe_3, and the phosphite, $P(OMe)_3$, and the series of (substituted arene)manganese tricarbonyl complexes (**IV**−**VII**) with reference to not only the regioselectivity between ring and metal attack, described in part A for the tropylium complexes (**I**−**III**), but also regioselectivity within the substituted arene ring. Calculated ΔE_{RS} values (Table 2) are again compared with low-temperature spectroscopic and synthetic studies summarized in Table 3. The ΔE_{RS} values were calculated as in part A and described further in the computational details section above. Again no major variation in order of relative interaction energies was found on either varying the extent of the CMO group or on varying the dielectric constant from 2 to 100, and thus the reactions between PMe_3, $P(OMe)_3$, and the series **IV**−**VII** are also predicted to be orbitally controlled as in part A.

Again the ΔE_{RS} value for exo ring attack is generally greater than the corresponding endo attack result and is also generally greater for PMe_3 than for $P(OMe)_3$, consistent with their relative nucleophilicities as discussed above in part A. However, in the case of the substituted arene complexes discussed here, it is noteworthy that the calculated interaction energies, both exo and endo, at the substituted carbon atoms are generally smaller than those at the unsubstituted carbon atoms thereby reflecting a greater repulsion between the substituted carbon atom and approaching nucleophile, even in the early transition state at 3 Å used in these calculations.

The values of the relative interaction energies for exo ring attack and metal attack for the arene complexes (**IV**−**VII**) are of interest. For example for PMe_3 attack on the toluene complex, **IV**, ring attack is predicted in agreement with experiment at low temperatures (see below). The order of predicted attack site is reversed for $P(OMe)_3$, again in agreement with experiment. In series A ring attack is always predicted for PMe_3 attack. In series B there is not such a clear preference for PMe_3 attack on the ring. The reasons for this difference between the two series of complexes in parts A and B is based on OMO−OMO interactions. As discussed in part A, metal attack by the nucleophile involves OMO−OMO repulsion between the nucleophile and substrate and the OMOs of $[(toluene)Mn(CO)_3]^+$ contain appreciable mixing of both ring and $Mn(CO)_3$ fragment orbitals in contrast to the tropylium complexes where the corresponding OMOs are more $M(CO)_3$ centered. For example the HOMO of $[(toluene)Mn(CO)_3]^+$ has 58% $Mn(CO)_3$, while that of $[(tropylium)Cr(CO)_3]^+$ has 80% $Cr(CO)_3$ (see Supporting Information). It follows that there is less repulsion between the approaching nucleophile and metal center and more repulsion for ring attack for the arene series (B) than for the tropylium series (A), and consequently metal attack occurs more readily for the arene series.

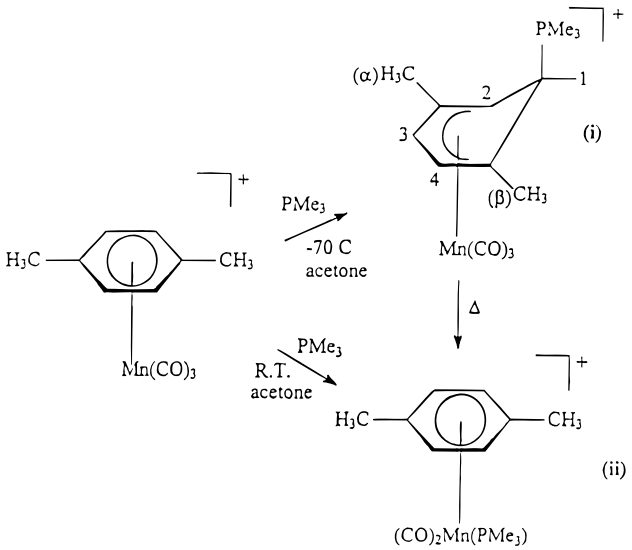

Figure 3. Scheme for the reaction of PMe_3 with $[(\eta^6\text{-}p\text{-}C_6H_4(CH_3)_2)Mn(CO)_3]^+$.

Detailed theoretical results are as follows: PMe_3 is predicted to give ring exo attack with the chlorobenzene, toluene, and p-xylene complexes (**VII**, **IV**, and **V**), while $P(OMe)_3$ is predicted to give metal attack with **IV** and **VII**. In the case of **IV**, PMe_3 is predicted to attack at the meta position (C_3).

Because of limitations on the number of atoms which can be included in the IDM approach, it was not possible to calculate interaction energies for attack by PMe_3 on the mesitylene cation (**VI**) nor by $P(OMe)_3$ on either the p-xylene (**V**) or the mesitylene cation (**VI**), so PMe_3 was modeled by PH_3 (Table 2). The fact that the calculated order of interaction energies for attack by PH_3 on the xylene complex (**V**) approximately parallels that for PMe_3 (Table 2) gives us confidence in comparing the calculated ΔE_{RS} values for PH_3 attacking the mesitylene cation (**VI**) with experimental results for PMe_3. Finally, the difference in calculated ΔE_{RS} values for PMe_3, giving ring attack for the toluene and p-xylene complexes (**IV** and **V**) but metal attack for mesitylene (**VI**) (modeled by PH_3 in this case), lies in the form of the UMOs which for **IV** and **V** are more ring centered than for **VI**, as well as on OMO−OMO repulsions (see Supporting Information).

Experimental Results. Reaction of PR_3 with $[(\eta^6\text{-}C_6H_{6-n}Me_n)Mn(CO)_3]PF_6$ (n =1 (IV), R = Me, OMe; n = 2 (V), R = Me, OMe; n = 3 (VI), R = Me, OMe) and $[(\eta^6\text{-}C_6H_5Cl)Mn(CO)_3]PF_6$ (R = Me, OMe). As an example, PMe_3 reacted with **V** in acetone at −60 °C to give immediately the ring adduct $[(\eta^5\text{-}C_6H_4Me_2\text{-}exo\text{-}PMe_3)Mn(CO)_3]PF_6$ (**XIV**) as evidenced by the appearance of ν(CO) peaks at 2019 and 1940 cm^{-1} and confirmed by the low-temperature ^1H NMR spectrum which showed resonances at δ 3.99 (m, H_1), δ 3.50 (m, H_2), δ 5.12 (d H_4, $J_{3,4}$ = 4.8 H_3), and δ 5.89 (br, H_5) with two singlets for the methyl groups at δ 1.70 (H_β) and δ 2.01 (H_α) and a doublet at δ 1.57 (J_{P-H} = 13.9 H_z) for the PMe_3 methyl (see Figure 2 for numbering scheme). On an increase of the temperature, carbonyl substitution occurred with formation of the stable $[(\eta^6\text{-}C_6H_4Me_2)Mn(CO)_2PMe_3]PF_6$ (**XV**) (Figure 3). Analytical data for **XV** and spectroscopic data for **XIV** and **XV** are given in Tables 4 and 5.

In contrast, $P(OMe)_3$ gave no reaction with **V** in acetone at low temperatures but on an increase of the

temperature the analogous carbonyl substitution product **XVI** formed.

In the case of the mesitylene complex (**VI**), neither PMe_3 nor $P(OMe)_3$ reacted in acetone at −60 °C but on an increase of the temperature monocarbonyl substitution occurred to give **XVII** and **XVIII**, respectively (data in Tables 4 and 5).

Comparison between Theoretical and Experimental Results. The ΔE_{RS} values indicate that PMe_3 is predicted to give ring attack with **IV**, **V**, and **VII** in excellent agreement with the above experimental results and those observed previously with PEt_3 as attacking nucelophile.[9] Moreover, the IDM approach also predicts correctly the isomer distributions for **IV** and **VII** observed in the PEt_3 studies, namely that **IV** gave solely meta addition (ΔE_{RS} for $C_3 = 13.6$, for $C_2 = 11.3$, and for $C_4 = 10.6$) whereas for **VII** a mixture of ortho/meta adducts (o:m = 2:1) were observed[9] which correlates with the theoretical values of $\Delta E_{RS}(C_3) = 15.3$ and $\Delta E_{RS}(C_2) = 15.2$. Finally, the calculated values of ΔE_{RS} for metal attack by $P(OMe)_3$ for **IV** and **VII** are always the largest values and so metal attack is predicted in agreement with the above experimental work.

Conclusions

Application of the interaction determinant method of calculating interaction energies between large nucleophiles such as PMe_3 and $P(OMe)_3$ and a series of π-acid metal carbonyl complexes provides excellent agreement with observed regio- and stereochemical control for both tropylium and substituted arene complexes, provided account is taken of the ranges of UMOs exhibited by both series of complexes.

Thus the IDM method correctly predicts exo ring addition as the initial site of attack by PMe_3 on complexes **I**−**III** and **IV**, **V**, and **VII** with, in the case of the toluene (**IV**) and chlorobenzene (**VII**) manganese tricarbonyl complexes a correct prediction of the ring substitution pattern (m for **IV** and o:m for **VII**). In the case of $P(OMe)_3$ the IDM method correctly predicts metal attack for **II**−**IV** and **VII**. These reactions are shown to be orbitally rather than charge controlled; however strong donor solvents such as THF result in specific solvation effects, consideration of which is not within the scope of the IDM approach.

Experimental Section

Solvents were freshly dried by standard methods. All reactions and workup were carried out under high-purity nitrogen. Tertiary phosphines and phosphites were obtained commercially and used without further purification. Infrared spectra were measured using a 0.1 mm CaF_2 cell on a Perkin-Elmer 1720 FT spectrometer linked to a 3700 data station and on a Mattson Galaxy FT300 spectrometer. Low-temperature spectra were recorded on a Specac variable-temperature cell (P/N 21 500). ^1H and ^{13}C NMR spectra were recorded on a Jeol GX 270 spectrometer. Analyses were performed by the Microanalytical Laboratory of the Chemical Services Unit of University College, Dublin. The starting complexes [(η^7-C_7H_7)$M(CO)_3$]BF_4 (**I**, M = Cr; **II**, M = Mo; **III**, M = W) and [(η^6-$C_6H_{6-n}(CH_3)_n$)$Mn(CO)_3$]PF_6 (n = 1−3) and [(η^6-ClC_6H_{5-n}-$(CH_3)_n$)$Mn(CO)_3$]PF_6 (n = 0, 1) were prepared by standard methods: **I**−**III**,[30] **IV**−**VII**.[31,32]

Typical Procedure for the Reaction between PMe_3 and [(η^7-C_7H_7)$Cr(CO)_3$]BF_4 (I). PMe_3 (0.12 g, 1.6 mmol) was added to a stirred solution of **I** (0.5 g, 1.6 mmol) in ethanol at −78 °C. An immediate color change from orange to dark red occurred. A sample was transferred by syringe to the precooled (−78 °C) low-temperature infrared cell and a spectrum taken immediately. New ν(CO) peaks appeared at 1990, 1935, and 1905 cm^{-1}. After the solution was stirred for 30 min, removal of solvent gave a violet residue which on recrystallization from CH_2Cl_2 gave the pure exo ring adduct [(η^6-C_7H_7-*exo*-PMe_3)$Cr(CO)_3$]BF_4 (**VIII**) (0.51 g, 81.2%). Similar procedures gave **IX**, **XI**, and related tungsten complexes. Analytical and spectroscopic data are given in Tables 4 and 5 and in the Supporting Information. In all cases the exo attack was confirmed from the ^1H NMR spectra (Table 5).

In the case of the reaction of $P(OMe)_3$ with **I**, the above procedure again gave the exo ring adduct **IX** (Tables 4 and 5), but with **II** no evidence could be obtained for ring addition; however, on warming of the sample to room temperature, filtration of decomposition products and subsequent chromatography on alumina and elution with CH_2Cl_2/acetone gave the pure ring-displaced product, *fac*-$(P(OMe)_3)_3Mo(CO)_3$ (**XII**). Further elution with CH_2Cl/acetonitrile (4:1) and recrystallization gave [(η^7-C_7H_7)$Mo(CO)_2P(OMe)_3$]BF_4 (**XIII**). Analytical and spectroscopic data are given in Tables 4 and 5. **III** behaved similarly (Supporting Information).

Reactions in THF. Using the above procedure, no color or infrared spectral changes occurred in the reactions of **I**−**III** with both PMe_3 and $P(OMe)_3$ at low temperatures; however, when the temperature was raised, workup, as described above, gave only the ring displaced products $(PR_3)_3M(CO)_3$ (see Tables 4 and 5 and Supporting Information).

Reactions in Toluene. Again **I**−**III** gave no evidence for reactions with PMe_3 and $P(OMe)_3$ at low temperature. On an increase of the temperature, **I** gave the ring-displaced product, whereas **II** and **III** gave carbonyl substitution [(η^7-C_7H_7)$M(CO)_2$-PR_3]BF_4 (M = Mo, W; R = Me, OMe).

Reactions of [(η^6-arene)$Mn(CO)_3$]PF_6 (IV−VII) with PR_3 (R = Me, OMe). The same general procedure for low-temperature studies was used as described above except for the use of acetone as solvent. For this series (**IV**−**VII**), attempts to isolate ring adducts at low temperatures were unsuccessful. A typical preparation of the carbonyl substitution product is as follows: PMe_3 (0.8 g, 1.12 mmol) was added to [(η^6-$C_6H_4Me_2$)$Mn(CO)_3$]PF_6 (0.25 g, 0.64 mmol) in acetone (30 mL) and reacted at room temperature for 1 h. After purification on alumina, removal of solvent and recrystallization from CH_2Cl_2/*n*-hexane gave yellow crystals of [(η^6-C_6H_4-Me_2)$Mn(CO)_2(PMe_3)$]PF_6 (**XV**) (0.21 g, 0.48 mmol, 73%). Other carbonyl substitution products (**XVI**−**VIII**) were obtained similarly. Analytical and spectroscopic data is given in Tables 4 and 5 and the Supporting Information.

Low-Temperature ^1H NMR Studies. A typical procedure is as follows: an NMR tube containing [(η^6-$C_6H_4Me_2$)$Mn(CO)_3$]-PF_6 in acetonitrile-d_3 was cooled to −30 °C (solution froze) and PMe_3 added, and the tube was immediately placed in the NMR probe cooled to −30 °C. The temperature was increased by 5 °C increments when the ring adduct was observed at −15 °C and was present up to room temperature when the carbonyl substitution product began to form.

Supporting Information Available: Tables giving analytical, infrared, and ^1H, ^{13}C, and ^{31}P NMR data for the complexes and intermediates in this study, together with LUMO−HOMO gaps, calculated charges, and overlap population and P_A^{LUMO} values of the series **I**−**VII** (29 pages). Ordering information is given on any current masthead page.

OM950962S

(30) Dauben, H. J.; Honnen, L. R. *J. Am. Chem. Soc.* **1958**, *80*, 5570.
(31) Winkhaus, L. P.; Wilkinson, G. *J. Chem. Soc.* **1961**, 3807.
(32) Pauson, P. L.; Segal, J. A. *J. Chem. Soc., Dalton Trans.* **1975**, 1677.